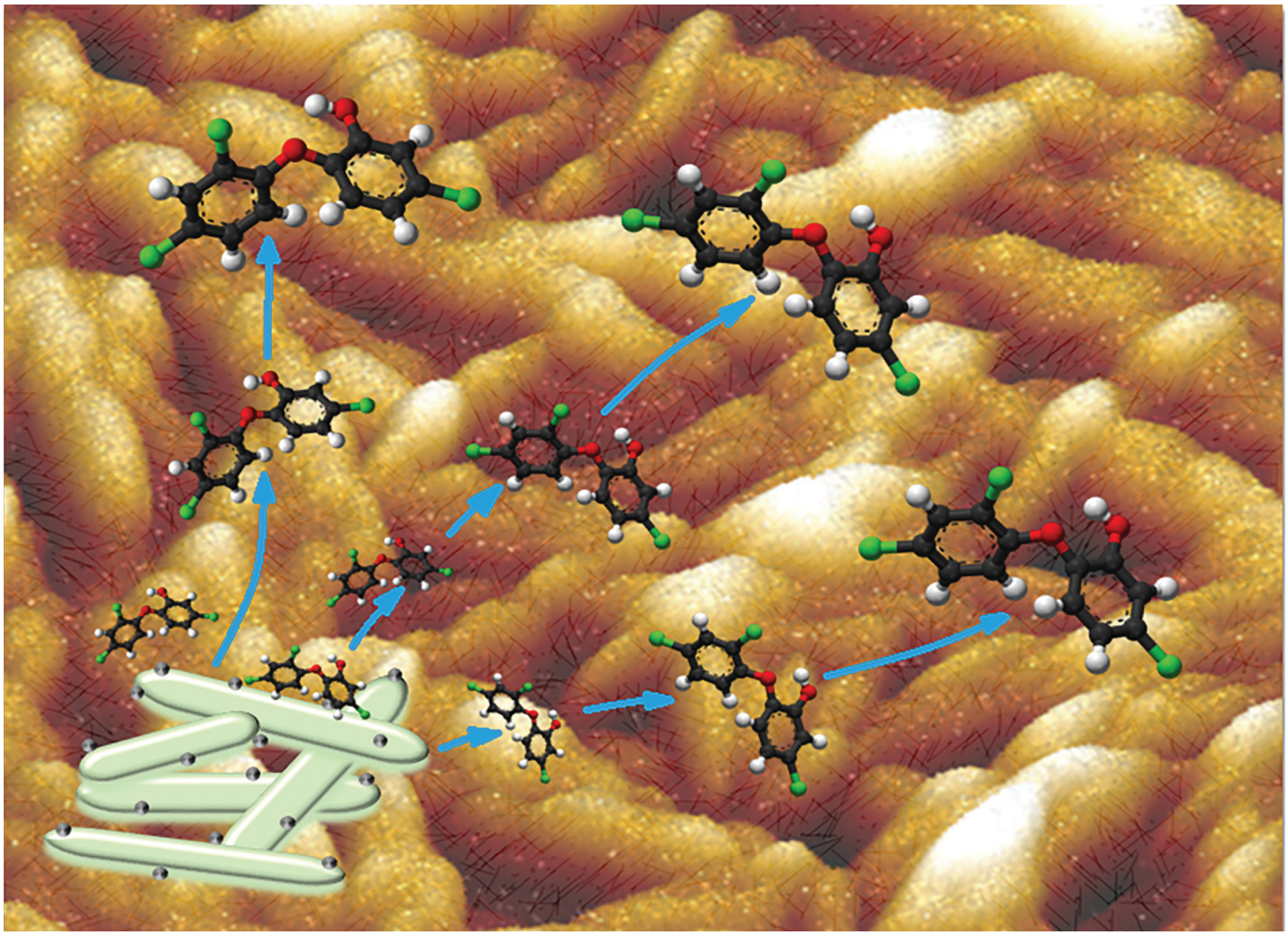

Showcasing research from Professors Seisenbaeva and Kessler laboratory, Department of Molecular Sciences, Uppsala BioCenter, Swedish University of Agricultural Sciences, Sweden.

Nanoceria–nanocellulose hybrid materials for delayed release of antibiotic and anti-inflammatory medicines

Nanoceria–nanocellulose hybrid material was developed and evaluated as a potential drug delivery system. Obtained materials possessed an open porous structure and absorbed pharmaceuticals *via* outer-sphere complexation mechanisms with ceria nanoparticles. Promising antibacterial properties and delayed release of antibiotic and anti-inflammatory medicines was observed.

As featured in:

See Vadim G. Kessler *et al.*, *Mater. Adv.*, 2022, **3**, 7228.

ROYAL SOCIETY OF CHEMISTRY

rsc.li/materials-advances

Registered charity number: 207890

Materials Advances

ROYAL SOCIETY OF CHEMISTRY

PAPER

View Article Online
View Journal | View Issue

Cite this: *Mater. Adv.*, 2022, 3, 7228

Nanoceria–nanocellulose hybrid materials for delayed release of antibiotic and anti-inflammatory medicines†

Servane Gaio,‡ Fredric G. Svensson,‡§ Troy C. Breijaert,‡ Gulaim A. Seisenbaeva and Vadim G. Kessler *

Received 26th April 2022,
Accepted 9th August 2022

DOI: 10.1039/d2ma00471b

rsc.li/materials-advances

A novel nanoceria–nanocellulose hybrid material has been developed and evaluated as a potential drug delivery system. Crystalline nanoceria was synthesized *in situ* in the nanocellulose to obtain a homogenous distribution without extensive particle aggregation. The hybrid materials were loaded with two antibiotic drugs, triclosan and ampicillin, and one anti-inflammatory drug, diclofenac. The bacteriostatic effect on the gram-negative bacteria *Escherichia coli* was evaluated for the hybrid materials containing triclosan and ampicillin. The nanoceria–nanocellulose hybrid displayed a better retention of ampicillin than triclosan in the disc diffusion test, which is likely due to the presence of the carboxylic acid group in ampicillin that has better affinity for ceria compared to the phenolic group in triclosan. However, drug release studies in solution revealed rapid release of ampicillin and diclofenac, indicative of outer-sphere complexes between ceria and the drugs.

Introduction

Wound management is critical in preventing infections and in facilitating healing processes. Traditional wound-dressings only act as a physical barrier to provide physical protection and prevent infection by microorganisms but they neither provide antibacterial properties nor do they promote the healing processes. These are called passive wound-dressings.[1] Recently, with the emergence of nanotechnology, a new type of wound-dressing has been the focus of a lot of research, the so called active wound-dressings. These active wound-dressings facilitate healing of the wound by exhibiting antibacterial properties and/or stimulate tissue regrowth.[2,3] For example, nanoparticles have been reported to improve wound healing by promoting immune responses.[4,5] Nanocellulose has been under intense investigation for use as a new bandage material, owing to numerous beneficial properties such as gas permeability, exudate removal, moist environment, ease of removal, possible templating effect for tissue regrowth, and pain relief.[6] There are three major classes of nanocellulose: crystalline nanocellulose (CNC), cellulose nanofibrills (CNFs), and bacterial cellulose (BC). CNC has dimensions of 5–20 nm × 100–500 nm and high crystallinity. CNFs are fibrous with a high aspect ratio and lengths up to *ca.* 1 μm. BC is synthesized by some bacteria and, like CNFs, the fibres are about 1 μm long.[7] The major drawback of all cellulose based materials, however, is the lack of antibacterial activity which means the wound could easily be infected. In efforts to overcome this, antibacterial agents have been added to the nanocellulose. For example, Volova *et al.*[8] produced bacterial cellulose-silver nanoparticle composites which demonstrated antibacterial effect *via* the release of silver ions. In other studies, drug release from chemically unmodified nanocellulose has been investigated.[2,9] In one study, Basu and co-workers[10] cross-linked CNFs with Ca^{2+} and Cu^{2+} ions. They found that Ca^{2+} appeared to inhibit biofilm production and Cu^{2+} ions had a negative effect on bacterial proliferation. Nanocellulose has low retention for antibiotics and there is a risk that a very quick release may have toxic effects. Several articles have reported the use of nanotitania–nanocellulose hybrid materials for controlled drug delivery,[11–13] where the good affinity of many common functional groups to the titania surface was exploited. Titania has for a long time been considered biocompatible with low toxicity. Lately, however, it has been demonstrated that titania induces very strong blood coagulation[5,14,15] which also can promote wound-healing by initiating immune responses.[5] For some applications, however, a strong coagulative response might be undesirable. Thus, we were interested in substituting nanotitania with nanoceria as a drug carrier in nanocellulose

Department of Molecular Sciences, Biocentrum, Swedish University of Agricultural Sciences, Almas Allé 5, SE-756 51 Uppsala, Sweden. E-mail: vadim.kessler@slu.se

† Electronic supplementary information (ESI) available. See DOI: https://doi.org/10.1039/d2ma00471b

‡ These authors contributed equally.

§ Present address: Department of Materials Science and Engineering, The Ångström Laboratory, Uppsala University, Lägerhyddsvägen 1, SE-75103 Uppsala, Sweden.

based wound-dressings. Cerium(IV) oxide (ceria, CeO_2) is generally considered a good biocompatible material with low toxicity and antioxidative properties owing to its non-stoichiometric composition.[16,17] The inherent ability to produce reactive oxygen species (ROS) of many nanoparticles (*e.g.* TiO_2, Ag, and Fe_3O_4) has been proposed to contribute to their cytotoxicity.[18] Ceria has been subjected to numerous and diverse biomedical studies.[19] For instance, Bellio and co-workers[20] used CeO_2 nanoparticles as adjuvants in combination with several antibiotics against multi-resistant *Klebsiella pneumonia*. They found an increased antibacterial activity from the antibiotics which is ascribed to disruptive interactions between the cell membrane and the CeO_2 nanoparticles. In another study, ceria nanosheets were found to have a higher antibacterial activity compared to ceria nanoparticles, which was ascribed to the higher surface area of the nanosheets.[21] Popov and co-workers[16] demonstrated a radioprotective effect of citrate-coated ceria nanoparticles. This effect was explained by the effective clearance of the formed hydrogen peroxide and hydroxyl radicals. The intake of citrate-capped ceria had a positive effect on the survival of mice exposed to X-ray radiation. Furthermore, drug delivery systems including ceria have been reported, for instance CeO_2–silicate composites.[22,23] However, to the best of the authors' knowledge, drug delivery from nanoceria–nanocellulose hybrid materials has yet not been reported. The aim of the current work was to investigate nanoceria–nanocellulose hybrid materials as a potential drug delivery system for two different antibiotics, ampicillin and triclosan, and the anti-inflammatory drug, diclofenac. Release rates were studied *in vitro* for ampicillin and diclofenac, while the bacteriostatic effect of the hybrid material containing triclosan and ampicillin was tested against a model bacterium, the gram-negative *E. coli*.

Materials and methods

Materials synthesis

Synthesis of CNC. In a typical procedure, 4 grams of raw cotton was suspended in 100 mL of *ca.* 64 weight% sulfuric acid at 50 °C under stirring for 1 hour to produce nanocrystalline nanocellulose (CNC). Then, the CNC slurry was immediately poured into 1 L of deionized (DI) water to quench the reaction. Once sedimented, the CNC was collected and concentrated by centrifugation. The CNC was transferred to a dialysis tube and stored in a large beaker with 4 L of deionized (DI) H_2O to increase the pH to approximately neutral by acid removal. The dry weight was then determined in the final CNC product by weighing the CNC slurry and CNC dried in an oven until constant weight. The as-synthesized CNC slurry was stored in tightly sealed containers prior to use.

Synthesis of ceria nanoparticles. Ceria nanoparticles were synthesized according to a modified literature procedure.[24] Cerium(IV) sulfate tetrahydrate (Merck, 98%) was dissolved in DI H_2O and added to the CNC suspension. The pH was then increased to *ca.* 9 by a drop-wise addition of 2 M NaOH. Thereafter the reaction mixture (RM) was stirred at 80 °C for 1 hour. The RM was repeatedly washed with DI H_2O and centrifuged until approximately neutral pH was reached followed by washing two times with ethanol (Solveco, 99.7%). The obtained powder was dried at 60 °C to obtain the low-temperature ceria (CeO_2_80), similar to the *in situ* synthesis of ceria in the CNC suspension. Some of this powder was annealed at 600 °C for 2 hours to obtain high-temperature ceria (CeO_2_600).

Modification of CNC/PEG with BTCA. The CNC was modified with 1,2,3,4-butanetetracarboxylic acid (BTCA, Aldrich, 99%) to act as an anchor for the metal oxide.[25] Briefly, for 1 g of CNC, 10 mmol BTCA and 10 mmol sodium hypophosphite (SHP, Aldrich, 99% (catalyst)) were dissolved in 1 mL 1 w% polyethylene glycol (PEG, Aldrich, 35 000 Da) and the RM was then stirred at 85 °C for 1 hour.

Modification of CNC/PEG/BTCA with CeO_2. To obtain a homogenous material with small ceria particles an *in situ* synthesis of ceria in the BTCA-modified CNC was performed. First, the pH of the CNC was increased to *ca.* 9 by the addition of ammonium hydroxide. Then, an appropriate amount of cerium(IV) sulfate hydrate was added to yield a final amount of 20 w% ceria. The RM was stirred at 80 °C for 30 min and was then poured into a Petri dish and placed in an oven at 60 °C until dry.

Modification with antibiotics. To modify the hybrid materials with the drugs, ampicillin (Sigma, >96%), triclosan (Sigma, >97%), or diclofenac (Sigma, >98%) dissolved in ethanol was added to the RM of CNC/BTCA or CNC/BTCA/CeO_2 under stirring. The suspensions were poured into Petri dishes and dried at 60 °C until dry. Pieces of hybrid material of 0.5 cm × 0.5 cm were produced (containing 0.2 mmol antibiotics per 0.25 cm^2 assuming homogenous distribution). For the chemical structure of the applied antibiotics, please, see Scheme 1.

Statistical tests. Significant differences between biological treatments were evaluated by Welch's two-sample *t*-test using R statistical software (version 3.4.3).[26] A *p*-value smaller than 0.05 was assumed to signify a statistically significant difference.

Materials characterization

Scanning electron microscopy. The morphology and homogeneity of all hybrid materials were studied by scanning electron microscopy (SEM, Hitachi TM1000 and Hitachi Flex-SEM1000II, Tokyo, Japan) coupled with energy-dispersive X-ray

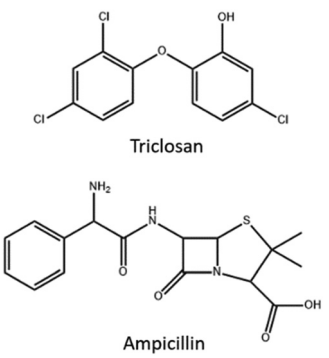

Scheme 1 Chemical structures of ampicillin and triclosan.

spectroscopy (EDS, Oxford Instruments, Abingdon, UK). Dry samples were mounted on carbon tape.

Nanoparticle tracking analysis. The particle size in the solution of the unmodified CNC was investigated using a Malvern Nanosight NS300 (Malvern, UK). CNC was diluted in DI H_2O and analyzed at an infusion rate of 100 μL in 20 s, recording fours series per sample.

Zeta-potential. A Malvern Zetasizer Nano (Worcestershire, UK) was used for dynamic light scattering (DLS) and zeta-potential measurements of pure CNC. 3 series of 30 measurements per sample were performed.

Atomic force microscopy. Measurements were done on a Bruker Dimension Fastscan AFM (Billerica, USA) in the ScanAsyst mode using Fastscan-B cantilevers at a scan rate of 3 Hz and 1024 samples per line. The data were processed using Gwyddion version 2.56, with align rows-median.

Powder X-ray diffraction. The crystallinity of the *in situ* synthesized ceria and CeO_2_80 and CeO_2_600 was investigated by powder X-ray diffraction. The ceria-containing material was freeze-dried and powdered and then put into glass capillaries with a diameter of 1 mm. X-Ray data collection was performed on a Bruker D8 SMART Apex II CCD diffractometer (Billerica, USA) with λ(Mo-Kα) = 0.71073 Å and a graphite monochromator. The Shelx97 program suite and EVA v12 were used for data treatment and analysis.

Fourier transform infrared spectrometry. The different materials were powdered by immersion in liquid nitrogen followed by grinding. The powders were milled in anhydrous KBr and pressed into pellets that were analysed by FTIR. The spectra were recorded using a PerkinElmer FTIR 100 spectrometer (Waltham, USA) between 4000 cm^{-1} to 400 cm^{-1} with 8 scans and 1 cm^{-1} resolution.

Photocatalytic studies. 10 mg of ceria nanoparticles, CeO_2_600 and CeO_2_80, were added to 1.5 mL of diluted methylene blue solution in plastic tubes. This was done in triplicate. These were kept in the dark for *ca.* 30 min to achieve adsorption-equilibrium. Then, the suspensions were centrifuged and absorbance was measured at 663 nm to obtain an initial absorbance using a Shimadzu UV-1800 spectrophotometer (Kyoto, Japan). After this, the solutions were subjected both to 300 W simulated sunlight (Osram) and a 15 W visible lamp (Garland) for periods of 15 min under gentle stirring. Subsequently, the solutions were centrifuged to sediment the ceria and then absorbance was measured. This was repeated three times for both treatments for a total of 45 minutes of irradiation time. The decomposition of MB was followed as the fraction of the initial absorbance.

Microbiological studies. Agar plates were prepared using Mueller Hinton broth powder (Sigma-Aldrich) at a concentration of 21 g L^{-1} in DI H_2O containing 1.5 w% agar (Sigma-Aldrich) powder, followed by autoclaving. *Escherichia coli* (*E. coli*, strain LMG8223) was grown in liquid Mueller Hinton medium overnight at 37 °C in the dark. An aliquot of the liquid bacteria culture was diluted 100 times in isotonic NaCl and subsequently spread on the agar plates. Then, a piece of hybrid material (0.5 × 0.5 cm) was placed in the centre of the agar plate. The agar plates were then incubated at 37 °C in the dark for 18 h to allow the bacteria to grow. The sizes of the inhibitory zones were then measured.

pH-Measurement of ampicillin addition to nanoceria–nanocellulose. For the pH-experiment was used a Metro Titrando 888 system, running TIAMO 2.5 control software, equipped with an 801 stirring unit and an Ecotrode Plus combined pH electrode. The combined pH electrode was calibrated using Sigma-Aldrich certified buffers prior to use. A sample of a CeO_2 composite material was produced as previously described until the addition of ampicillin. Afterwards the composite was transferred to a suitable vessel equipped with a stirring bar, placed on the stirring unit, fitted with a thoroughly rinsed pH electrode, and allowed to equilibrate with stirring for 1 minute prior to starting the measurement. Under stirring the sample was then allowed to equilibrate for 120 seconds, measuring at 2 second intervals before the addition of ampicillin after which the change of pH was recorded for a total of 900 seconds at 2 second intervals.

Results and discussion

The aim of the current study was to investigate the nanocellulose–nanoceria hybrid as potential new materials for controlled drug delivery in wound-dressings, where nanoceria was evaluated as a substitute for nanotitania as a drug-carrier.

CNC synthesis

CNC was synthesized *via* acid hydrolysis from raw cotton. The average fiber sizes of the unmodified CNC were determined by AFM and NTA.

Atomic force microscopy

Diluted suspensions of unmodified CNC were analyzed by AFM to determine particle size and morphology (Fig. 1 and Fig. S2–S4, ESI†). As shown in Fig. 1, the CNC fibers have rod-like morphology, with a calculated average length of 112 nm (standard deviation 36 nm) and an average width of 48 nm (standard deviation 13 nm).

NTA and zeta-potential

Dilute suspensions of unmodified CNC were analysed by NTA (Fig. 2). The average particle size in solution was 113 nm, which is in good agreement with the AFM results. There are pieces of evidence for aggregation in solution. The zeta-potential of unmodified CNC was determined to be 2.44 ± 0.85 mV.

CNC modification

Polyethylene glycol (PEG) was added to CNC to increase the strength of the final material. To get better retention of the ceria nanoparticles, the CNC was modified by BTCA to introduce carboxylic functions to which the ceria nanoparticles can attach. Transmission FTIR spectra were recorded for freeze-dried powdered materials (Fig. 3). An absorption band around 1160 cm^{-1} is assigned to the C–O–C bonds in the CNC. With the introduction of BTCA a vibration from the carbonyl groups appears at 1712 cm^{-1}. When ceria is added the carbonyl band is

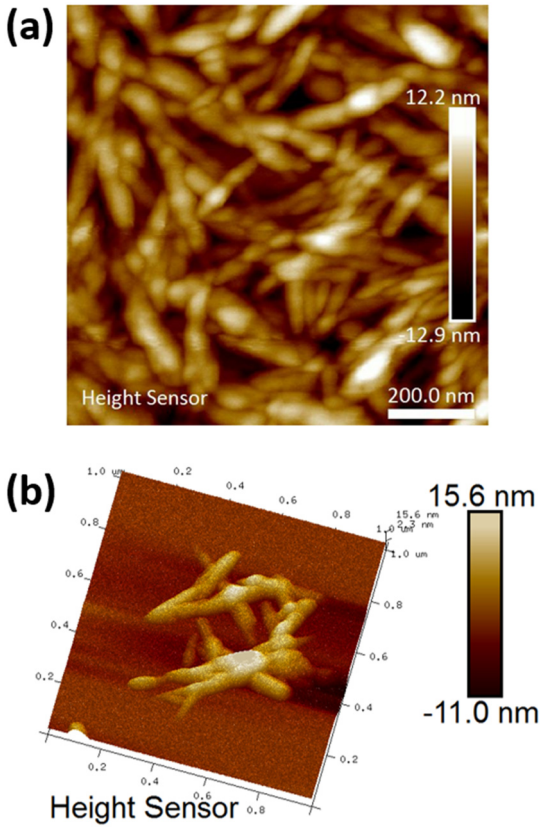

Fig. 1 (a) 2D AFM micrograph of the unmodified CNC and (b) 3D micrograph of unmodified CNC fibres.

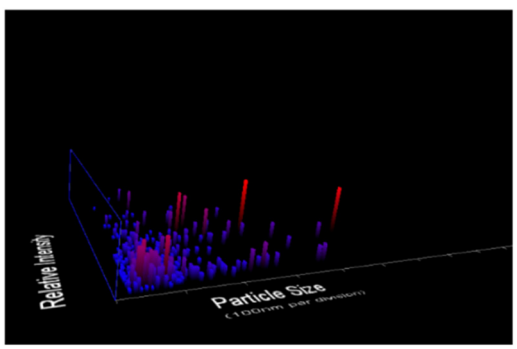

Fig. 2 NTA measurements of diluted aqueous suspension of CNC, showing size distributions. The four different trial analyses have shown a mean CNC particle size of 113 nm with a standard deviation of 97 nm.

slightly shifted to 1708 cm^{-1}, indicating interaction between CeO_2 and the carboxylic group. Additionally, two bands assigned to Ce–O vibrations emerged at 465 cm^{-1} and 617 cm^{-1}.[27]

SEM imaging of the hybrid materials

The morphologies of the hybrid materials were visualized by SEM analysis. The hybrid materials had increased surface roughness (Fig. 4) compared to the unmodified CNC/PEG, which have a very smooth surface (Fig. S1a, ESI†). This increase

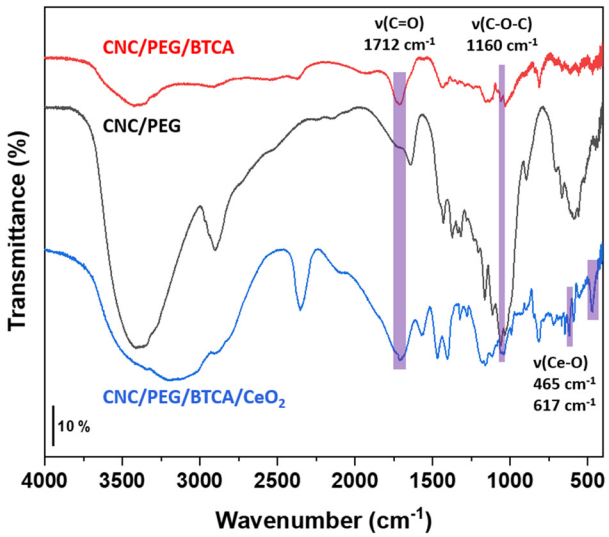

Fig. 3 FTIR spectra of powdered CNC/PEG, CNC/PEG/BTCA, and CNC/PEG/BTCA/CeO_2. Key absorption bands are highlighted.

in roughness is explained by the modification of BTCA and formation of ceria nanoparticles inside the materials. The addition of pre-synthesized ceria nanoparticles to the CNC/PEG suspension resulted in large aggregates of ceria unevenly distributed over the surface (Fig. S1b, ESI†). Instead, changing to an *in situ* synthesis of nanoceria in the CNC/PEG/BTCA resulted in a very good dispersion of the nanoparticles, without any visible aggregates, as clearly seen in Fig. 4.

Characterization of the nanoceria

To obtain a material of higher homogeneity and with smaller ceria particles an *in situ* low-temperature synthesis of ceria from cerium(IV) sulfate in the modified nanocellulose suspension was employed. The formation of nanocrystalline cerianite–CeO_2 in the CNC was confirmed by PXRD analysis of the hybrids. Fig. 5a shows the PXRD diffractogram of low-temperature ceria and Fig. 5b shows the diffractogram of ceria synthesized in BTCA-modified CNC. The size of low-temperature ceria was investigated by AFM, revealing a rather homogenous size distribution with particles of about 30 nm in diameter (Fig. 6 and Fig. S5 through S7, ESI†).

Photocatalytic studies

It is desirable to use in the wound dressings a metal oxide with low ROS production to avoid potential cell damage from the wound dressings. Thus, the photocatalytic activities of low-temperature ceria and ceria annealed at 600 °C were investigated by following the decomposition of methylene blue (MB) under two different light sources, 300 W simulated sunlight and a 15 W lamp (Fig. 7). MB solutions without catalyst powder were used as the control. It was found that the overall degradation of MB was very small for all treatments, with more than 90% of the initial concentration remaining after 45 min of irradiation. The degradation of MB was slightly larger for the low-temperature ceria which could be explained by a larger total active surface area

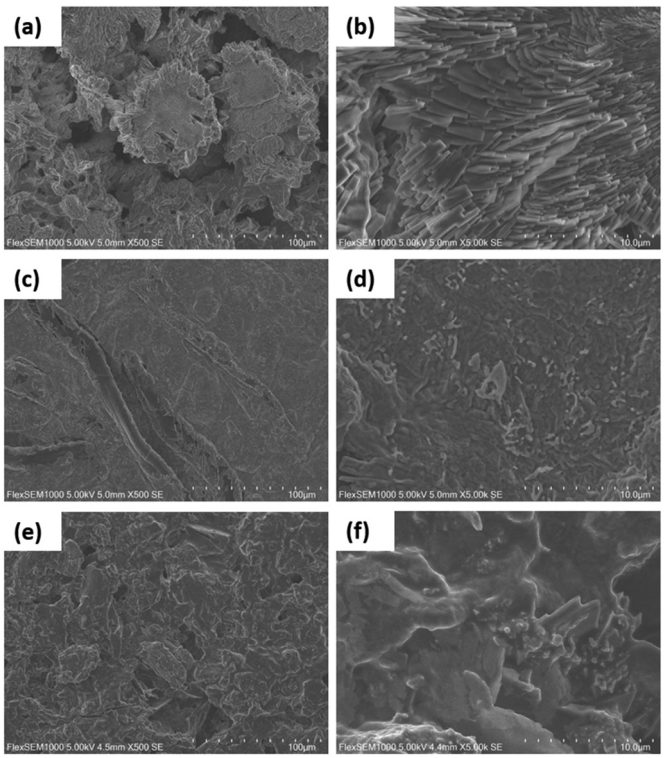

Fig. 4 SEM micrographs of CNC/PEG/BTCA/CeO_2/ampicillin at 500× (a) and 5000× (b) magnification, CNC/PEG/BTCA/CeO_2/triclosan at 500× (c) and 5000× (d) magnification, and CNC/PEG/BTCA/CeO_2/diclofenac at 500× (e) and 5000× (f) magnification.

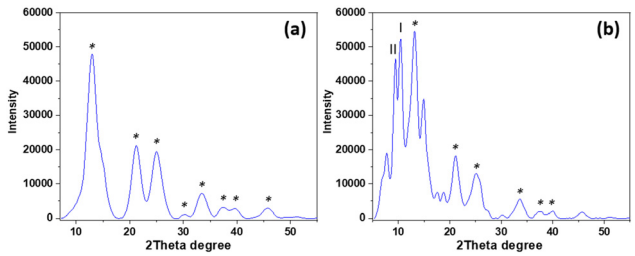

Fig. 5 PXRD diffractogram of (a) low-temperature ceria and (b) ceria synthesized *in situ* in CNC. The asterisk indicates characteristic diffraction planes of ceria (JCPDS 00-034-0394). Diffractions at 13.08°, 21.42°, 25.14°, 30.24°, 33.54°, 37.74°, 39.84°, and 45.84° represent the (1 1 1), (2 2 0), (3 1 1), (4 0 0), (3 3 1), (4 2 2), and (5 1 1) planes, respectively, of cerianite–CeO_2. Two characteristic diffractions of cellulose are present, where I represents the (2 0 0) plane of cellulose-I and II represents the (1 0 −1) plane of cellulose-II.[12]

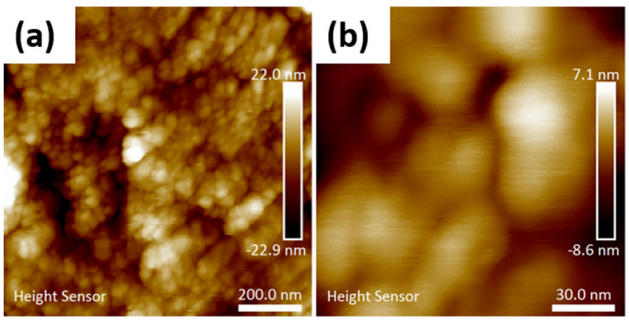

Fig. 6 (a) AFM micrograph of low-temperature nanoceria (CeO_2_80), and (b) high magnification micrograph of low-temperature nanoceria (CeO_2_80).

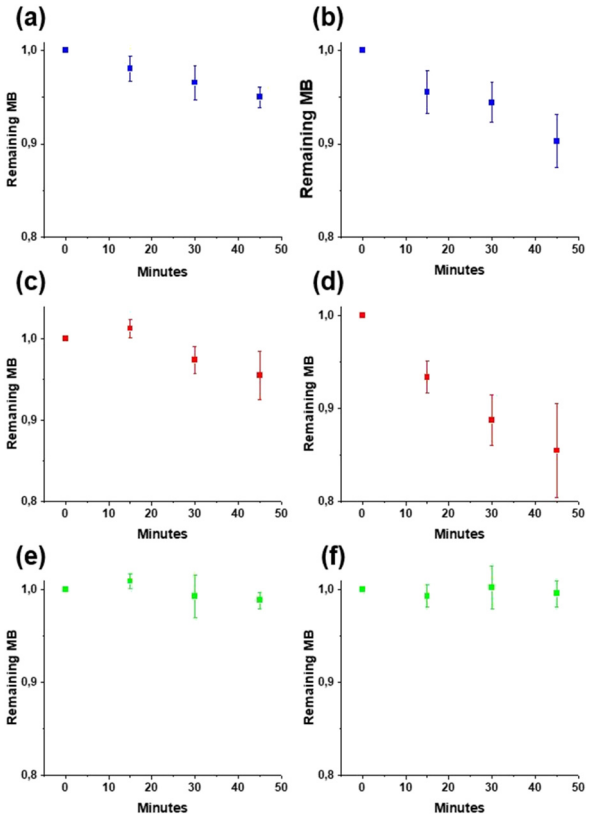

Fig. 7 Photocatalytic decomposition of methylene blue under a 15 W lamp: MB (a), CeO_2_80 (c), and CeO_2_600 (e) and 300 W simulated sunlight: MB (b), CeO_2_80 (d), and CeO_2_600 (f). The diagrams show the fraction of remaining MB after 45 min of irradiation time. Error bars represent standard deviation.

compared to the ceria annealed at 600 °C, as extensive particle aggregation and crystallite growth occur during annealing at high temperatures. In the current study, the photocatalytic activities of both the low-temperature and the high-temperature ceria were very low and this suggests ROS production in the nanoceria–nanocellulose hybrid should be negligible.

Release studies of ampicillin and diclofenac

Release of ampicillin and diclofenac from CNC/PEG and CNC/PEG/BTCA/CeO_2 was studied. The two drugs were almost completely released within 15 minutes (Table 1) for both materials, indicating they were not strongly interacting with the ceria nanoparticles. This is in sharp contrast to diclofenac adsorbed to nanotitania–nanocellulose composites in which only 50% released after 16 hours or 28% after 15 hours, depending on the preparation method, as a result of strong complexation with the titania surface.[12]

This is further supported by the pH-measurements where upon addition of ampicillin a small, temporary downward shift

Table 1 Release data for diclofenac and ampicillin from CNC/PEG and CNC/PEG/CeO_2

	CNC/PEG	CNC/PEG/CeO_2
Diclofenac drug loading	15.95 mg g^{-1}	11.7 mg g^{-1}
Diclofenac drug release	85–90% in 15 min	75–85% in 15 min
Ampicillin drug loading	15.98 mg g^{-1}	8.9 mg g^{-1}
Ampicillin drug release	85–100% in 15 min	85–100% in 15 min

in pH is measured after which the pH equilibrates to the previously measured value. This indicates that ampicillin is quickly transformed into the anionic form and consequently the interaction between the drug and ceria would be *via* the formation of an outer-sphere complex.

Microbiological studies

The inhibitory effect on the growth of *E. coli* was tested for the different materials *via* the disc diffusion test. The distance between the edge of the film and the end of the inhibitory zone was measured. CNC/PEG had negligible activity. The BTCA modified CNC had a certain antibacterial effect, which has been noticed previously for our CNC–TiO_2 system, originating from unbound/hydrolyzed BTCA.[13] CNC/PEG/BTCA/CeO_2 has substantially a lower antibacterial activity compared to CNC/PEG/BTCA. This is likely due to the adsorption of BTCA on the ceria nanoparticles *via* its carboxylic groups. Thus, the influence of BTCA on the antibacterial activity in the ceria containing materials should be small. Modification with two different antibiotics, triclosan and ampicillin, was then tested. There were clear differences in the retention capacity between them, where ampicillin was released much more slowly in comparison to triclosan in gel diffusion on a Petri dish (Fig. 8 and Fig. S9, ESI†). The inhibitory zone of CNC/PEG/CeO_2/ampicillin was significantly smaller ($p \ll 0.05$) compared to that of CNC/PEG/ampicillin while the difference between CNC/PEG/BTCA/triclosan and CNC/PEG/BTCA/CeO_2/triclosan was non-significant. This is likely explained by the presence of a carboxylic acid group in ampicillin which has better affinity for the ceria surface compared to the hydroxyl group in triclosan. This is also supported by the adsorption of BTCA on ceria. The release of ampicillin and diclofenac in 0.9% NaCl solution was studied by UV-spectrometry. Almost a 100% release was observed after *ca.* 15 minutes. The difference in retention of ampicillin in solution and in gel experiments can be supposedly attributed to the combination of the weakening of hydrogen bonding in the excess of aqueous medium and the mechanical washing. Complexation between ceria and the ligands appears to proceed in the form of outer-sphere complexes in contrast to complexation with titania, where inner-sphere surface complexes were easily traceable by FTIR and the release was rather apparently prolonged in time also in solution.[12,13] It should be noted, however, that gel diffusion is more relevant as a model for drug delivery on skin and thus the developed material can be considered promising.

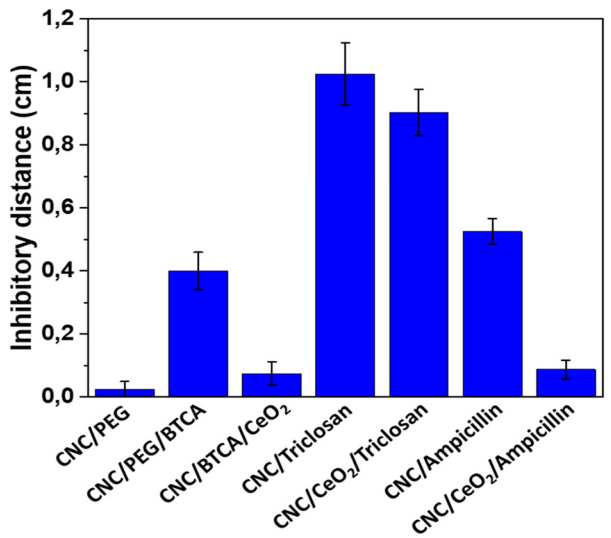

Fig. 8 Average inhibitory effect of the different materials. Error bars represent standard error of mean. At least eight replicates were made for each material. CNC/PEG/BTCA/CeO_2, CNC/PEG/BTCA/triclosan, CNC/PEG/BTCA/CeO_2/triclosan, CNC/PEG/BTCA/ampicillin, and CNC/PEG/BTCA/CeO_2/ampicillin have been abbreviated in the figure as CNC/BTCA/CeO_2, CNC/triclosan, CNC/CeO_2/triclosan, CNC/ampicillin, and CNC/CeO_2/ampicillin.

Conclusions

In this work we have developed a novel nanocellulose–nanoceria hybrid material and evaluated it for drug delivery for two different antibiotics, ampicillin and triclosan, against *E. coli*. It was found that ampicillin was released much slower than triclosan in the gel diffusion experiment, which was attributed to the strong interaction between its carboxylic group and nanoceria. However, rapid and almost complete release of ampicillin and diclofenac within 15 minutes in solution indicate weaker electrostatic interaction between the drugs and nanoceria, as compared to nanotitania where the drugs bond to the surfaces. No appreciable photocatalytic activity was found from the ceria nanoparticles under different visible light radiation sources, which suggests that production of harmful ROS is limited.

Author contributions

Investigation and analysis: S. G.; supervision, analysis, conceptualization, and writing – original draft preparation: F. G. S.; investigation and analysis: T. C. B.; writing – review and editing: G. A. S.; funding acquisition, conceptualization, and writing – review and editing: V. G. K.

Funding

This research was funded partly by the Swedish Research Council (Vetenskapsrådet) grant number 2014-3938 and partly by the Swedish Research Council STINT grant Nanocellulose Based Materials for Environmental and Theranostic Applications.

The Faculty of Natural Resources and Agricultural Sciences, SLU, is acknowledged for support of TB PhD position.

Conflicts of interest

The authors declare no conflicts of interest.

Acknowledgements

We thank Rasmus Björk for assistance with the DLS and zeta-potential measurements and Dr Jolanta Levenfors for kindly providing the *E. coli* bacteria. S. G. is grateful to the Erasmus+ Programme for financing her stay at SLU.

References

1 A. E. Stoica, C. Chircov and A. M. Grumezescu, *Molecules*, 2020, **25**, 2699.
2 S. Moritz, C. Wiegand, F. Wesarg, N. Hessler, F. A. Muller, D. Kralisch, U. C. Hipler and D. Fischer, *Int. J. Pharm.*, 2014, **471**, 45–55.
3 M. Li, Y. P. Liang, J. H. He, H. L. Zhang and B. L. Guo, *Chem. Mater.*, 2020, **32**, 9937–9953.
4 J. Tian, K. K. Y. Wong, C. M. Ho, C. N. Lok, W. Y. Yu, C. M. Che, J. F. Chiu and P. K. H. Tam, *ChemMedChem*, 2007, **2**, 129–136.
5 G. A. Seisenbaeva, K. Fromell, V. V. Vinogradov, A. N. Terekhov, A. V. Pakhomov, B. Nilsson, K. N. Ekdahl, V. V. Vinogradov and V. G. Kessler, *Sci. Rep.*, 2017, **7**, 15448.
6 M. Jorfi and E. J. Foster, *J. Appl. Polym. Sci.*, 2015, **132**, 41719.
7 T. Abitbol, A. Rivkin, Y. F. Cao, Y. Nevo, E. Abraham, T. Ben-Shalom, S. Lapidot and O. Shoseyov, *Curr. Opin. Biotechnol.*, 2016, **39**, 76–88.
8 T. G. Volova, A. A. Shumilova, I. P. Shidlovskiy, E. D. Nikolaeva, A. G. Sukovatiy, A. D. Vasiliev and E. I. Shishatskaya, *Polym. Test.*, 2018, **65**, 54–68.
9 E. Haimer, M. Wendland, K. Schlufter, K. Frankenfeld, P. Miethe, A. Potthast, T. Rosenau and F. Liebner, *Macromol. Symp.*, 2010, **294-II**, 64–74.
10 A. Basu, K. Heitz, M. Stromme, K. Welch and N. Ferraz, *Carbohydr. Polym.*, 2018, **181**, 345–350.
11 O. L. Galkina, K. Onneby, P. Huang, V. K. Ivanov, A. V. Agafonov, G. A. Seisenbaeva and V. G. Kessler, *J. Mater. Chem. B*, 2015, **3**, 7125–7134.
12 O. L. Galkina, V. K. Ivanov, A. Agafonov, G. A. Seisenbaeva and V. G. Kessler, *J. Mater. Chem. B*, 2015, **3**, 1688–1698.
13 O. L. Evdokimova, F. G. Svensson, A. V. Agafonov, S. Hakansson, G. A. Seisenbaeva and V. G. Kessler, *Nanomaterials*, 2018, **8**, 228.
14 B. Ekstrand-Hammarstrom, J. Hong, P. Davoodpour, K. Sandholm, K. N. Ekdahl, A. Bucht and B. Nilsson, *Biomaterials*, 2015, **51**, 58–68.
15 F. G. Svensson, V. A. Manivel, G. A. Seisenbaeva, V. G. Kessler, B. Nilsson, K. N. Ekdahl and K. Fromell, *Nanomaterials*, 2021, **11**, 1100.
16 A. L. Popov, S. I. Zaichkina, N. R. Popova, O. M. Rozanova, S. P. Romanchenko, O. S. Ivanova, A. A. Smirnov, E. V. Mironova, I. I. Selezneva and V. K. Ivanov, *RSC Adv.*, 2016, **6**, 106141–106149.
17 P. Roberta, S. E. Maria, I. Carmelo, C. Fabiano, R. M. Teresa, I. Sara, S. Antonio, F. Roberto, I. Giuliana and B. M. Violetta, *Toxicol. Res.*, 2021, **10**, 570–578.
18 F. Marano, S. Hussain, F. Rodrigues-Lima, A. Baeza-Squiban and S. Boland, *Arch. Toxicol.*, 2011, **85**, 733–741.
19 A. B. Shcherbakov, V. V. Reukiv, A. V. Yakimansky, E. L. Krasnopeeva, O. S. Ivanova, A. L. Popov and V. K. Ivanov, *Polymers*, 2021, **13**, 924.
20 P. Bellio, C. Luzi, A. Mancini, S. Cracchiolo, M. Passacantando, L. Di Pietro, M. Perilli, G. Amicosante, S. Santucci and G. Celenza, *Biomembranes*, 2018, **1860**, 2428–2435.
21 F. Abbas, J. Iqbal, T. Jan, N. Badshah, Q. Mansoor and M. Ismail, *Int. J. Miner., Metall. Mater.*, 2016, **23**, 102–108.
22 J. H. Zhang and Y. F. Zhu, *Microporous Mesoporous Mater.*, 2014, **197**, 244–251.
23 C. Xu, Y. H. Lin, J. S. Wang, L. Wu, W. L. Wei, J. S. Ren and X. G. Qu, *Adv. Healthcare Mater.*, 2013, **2**, 1591–1599.
24 O. Yildiz, *J. Nucl. Mater.*, 2007, **366**, 266–271.
25 O. L. Galkina, A. Sycheva, A. Blagodatskiy, G. Kaptay, V. L. Katanaev, G. A. Seisenbaeva, V. G. Kessler and A. V. Agafonov, *Surf. Coat. Technol.*, 2014, **253**, 171–179.
26 R Core Team, A Language and Environment for Statistical Computing; R Foundation for Statistical Computing, Vienna, Austria, 2016.
27 O. Ejeromedoghene, O. Oderinde, X. Y. Ma, M. Olusola, S. Adewuyi and G. D. Fu, *J. Mater. Sci.: Mater. Electron.*, 2021, **32**, 16324–16334.